GAS FLOODING OF AN INCLINED BLADE IMPELLER*

Václav MACHOŇ[a], Ivan FOŘT[b], Eva ANTOŠOVÁ[c], Bohumil ŠPANIHEL[c] and Vladimír KUDRNA[a]

[a] *Department of Chemical Engineering, Prague Institute of Chemical Technology, 166 28 Prague 6*
[b] *Department of Chemical and Food Process Equipment Design, Czech Technical University, 166 07 Prague 6*
[c] *Fat Industry, Research Institute, 145 00 Prague 4*

Received February 23, 1990
Accepted May 7, 1990

The conditions are studied in the paper of flooding the six plane blade impeller with blades inclined at the angle of 45° of relative size $d/D = 1/3$ and relative distance from the bottom of cylindrical vessel $H_2/D = 1/3$ equipped at the wall with four radial baffles of width $b/D = 0{\cdot}1$ at the relative vessel filling $H/D = 1$. The flooding conditions are determined experimentally from the course of dependence of the power input ratio of gassed and ungassed impeller on the flow rate number of air blown into the liquid phase (water) in the vessel. Theoretically, the conditions of the impeller flooding, when it is no more able to disperse air blown into the charge, are determined from balance of forces in the liquid flow leaving the region of rotating impeller acting on the bubbles of rising gas under the turbulent regime of charge flow. The results of the blade impeller frequency of revolutions determined theoretically at its flooding were found to be in good agreement with the experimentally determined values of the frequency of revolutions investigated obtained in the model equipment with vessel diameter $D = 290$ mm.

Agitating of microbial suspensions in fermentors plays an important role when intensifying the mass and heat transfer in agitated charge. The three phase system liquid (nutrient solution)–gas(air)–solid phase (microbial or other culture) is concerned here. For an intensive mixing of all these three phases, axial high-speed impellers, e.g., inclined plane blade impellers[1,2] are recommended which bring about largely axial flow[3] from the rotor region of impeller (i.e., the imaginary cylinder formed by rotating impeller blades). These impellers bring about a vigorous charge macroflow[3,4] and, in addition to it, an intensive mass (oxygen) transfer into the liquid phase[1]. Unlike agitating by radial high-speed impellers[5] (e.g., by a standard turbine impeller), which mechanically cause a stress of present microorganisms and so reduce their production, the axial high-speed impellers act more softly[1,4] on the

* Part LXXVIII in the series Studies on Mixing; Part LXXVII: Collect. Czech. Chem. Commun. *54*, 2345 (1989).

present microorganisms. It refers especially the filamentous (myceliar) suspensions e.g., in the production of citric acid, antibiotics, etc.

The gas flooding of impeller[6] was defined as the conditions when the mechanical impeller is not able, at the given frequency of revolution n, to disperse air (gas) of volumetric flow rate V_g blown into the agitated charge. The relation between quantities n and V_g was determined experimentally, e.g. refs[6-8], for the standard (Rushton) turbine impeller, and the resulting relations were expressed in terms of dimensionless criteria of similarity – flow rate number N_F and Froude number for mixing Fr_M. Experimental techniques were used, either direct[6] (conductivity measurement) or indirect[7-9] when the flooding conditions were determined from the course of curves $P_g/P_o = f(N_F)$. Similar experimental study[10] had been carried out also with the six inclined (at angle $\alpha = 45°$) plane blade impeller ($h = 0{\cdot}2d$) (ref.[11]) – see Fig. 1, however, the frequency of impeller revolutions had not been accessed quantitatively there. It had been only revealed that minima had manifested themselves on the given dependence in the course of curve $P_g/P_o = f(N_F)$, when the so-called large cavities behind the impeller blades had ceased to be stable, and the impeller flooding with air had taken place.

THEORETICAL

A system is considered (see Fig. 2) consisting of a flat-bottomed cylindrical vessel

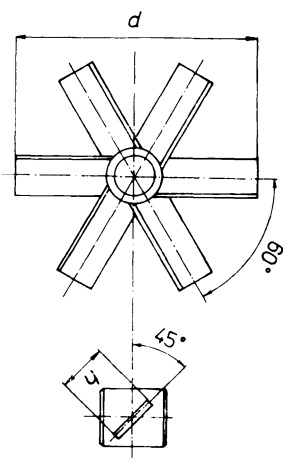

FIG. 1
Six plane blade impeller with inclined blades (pitched blade turbine)

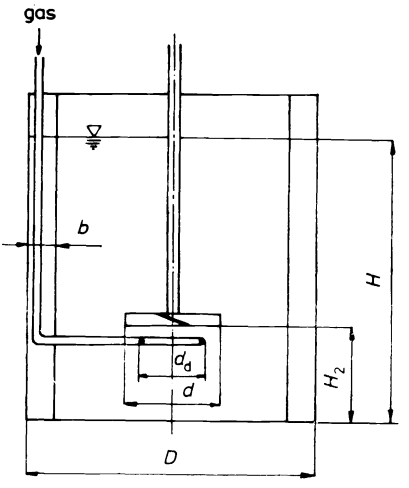

FIG. 2
Apparatus scheme

equipped with radial baffles at its wall. In this system rotates an axial high-speed impeller located axially in such a way that it pumps liquid towards bottom. Under the impeller, a sparger ring (distributor) is placed axially as well whose diameter is smaller than that of impeller; by this distributor, gas (air) is blown into the system.

When deriving the flooding conditions, we start from the fact that the liquid streaking out of the impeller with axial effect flows to the vessel bottom. At a constant impeller frequency of revolutions and at low flow rates of gas, bubbles of small diameter are formed which are carried along with liquid to the bottom, and the gas is dispersed in the charge in the way which is termed in the literature[10] as indirect dispersion (loading). With increasing gas flow rate, the bubble diameter grows and so does also the buoyancy force acting on the bubble. The bubbles rise upwards to the impeller, coalesce under the impeller, get to the close vicinity of impeller blades, and this situation is termed as direct dispersion[10] (loading). On further increasing the gas flow rate, the bubble passage through the impeller rotor region takes place, and the gas rises along the shaft without dispersing. This situation is termed as the gas flooding of impeller.

When describing quantitatively the flooding conditions, we started from the following pattern: two forces of opposite direction act on the bubble rising from the sparger ring. Upwards it is the buoyancy force and against it, the force of drag of liquid streaking from the impeller. The buoyancy force must be higher than the force of drag of streaking liquid for the bubble to permeate the impeller rotor region. The following derivation of critical conditions, at which just the impeller flooding occurs, is based on the idea that this phenomenon occurs at equality of buoyancy and drag forces acting on the bubble, consequently: buoyancy force = drag force which is put up to bubble by the liquid streaking from the impeller:

$$\tfrac{1}{6} g \pi d_b (\varrho_l - \varrho_g) = \psi \varrho_l \tfrac{1}{4} \pi d_b^2 \tfrac{1}{2} \omega^2 , \qquad (1)$$

where d_b is the bubble diameter and ψ the drag coefficient. The mean velocity of iquid leaving the rotor region of impeller can be determined in terms of : he relation

$$\omega = V_P S^{-1} , \qquad (2)$$

where the circular cross section taken up by the rotating impeller

$$S = \pi d^2/4 \qquad (3)$$

and the volumetric flow rate of liquid through the impeller (the impeller pumping capacity)

$$V_P = C_P n d^3 . \qquad (4)$$

Constant C_P depends on the type and size of impeller, on its position, on the height of liquid level at rest and on the Reynolds number for mixing, Re_M (ref.[12]). In our arrangement and for the turbulent flow region, according to literature[12] $C_P \cong 1$; for the six blade impeller with inclinded plane blades ($\alpha = 45°$), $d/D = H_2/D = 1/3$, $h/D = 0{\cdot}2$, $Re_M > 1{\cdot}0 \,.\, 10^3$ (see Fig. 1). After substituting we get

$$\omega = 4\pi^{-1} C_P n d \,, \tag{5}$$

and for the value of Reynolds number Re_b for the flow around the bubble

$$Re_b = \omega d_b \nu^{-1} = 4\pi^{-1} C_P n d d_b \nu^{-1} \,. \tag{6}$$

For further solution we insert the numerical values for the actual conditions. On using water as a liquid at 20°C and the diameter of the axial high-speed impeller used by us (see Fig. 1), we get

$$Re_b = 1{\cdot}26 \,.\, 10^5 n d_b \,. \tag{7}$$

Drag coefficient ψ is constant in the turbulent region of flow around the bubble by liquid ($Re_b > 1{\cdot}0 \,.\, 10^3$). Considering the lowest frequency of revolutions, which was used in our experiments, $n = 4\ s^{-1}$, the bubble diameter d_b should have to be smaller than $1{\cdot}98 \,.\, 10^{-3}$ m, then the turbulent region should be concerned. The existence of such small bubbles in the system which does not have expressively noncoalescent properties, is not real, therefore we assume coefficient ψ to be constant. Its value is considered in agreement with literature[13] to be $\psi = 0{\cdot}44$. The bubble diameter d_b depends on the gas volumetric flow rate, and we have taken relation[14] from the literature for the gas volume in bubble:

$$V_b = 1{\cdot}378 V_g^{1.2} g^{-0.6} \,. \tag{8}$$

On the assumption of spherical shape of bubbles, their mean diameter is then

$$d_b = 0{\cdot}874 V_g^{0.4} \,. \tag{9}$$

After inserting Eqs (5) and (9) into Eq. (1) we obtain the dependence between the critical frequency of impeller revolutions and the diameter of bubbles

$$n_{c,th} = (1{\cdot}99 \,.\, 10^3 d_b)^{0.5} \,. \tag{10}$$

The resulting equation for the calculation of the lowest frequency of revolutions at which the impeller flooding does not take place yet is

$$n_{c,th} = 41{\cdot}68 V_g^{0{\cdot}2} \,. \qquad (11)$$

From Eq. (*11*) it is possible to calculate the lowest impeller frequency of revolutions n_c for the given flow rate of gas V_g at which the gas does not permeate through the rotor region of the chosen type and size of axial high-speed impeller. In harmony with our hypothesis, these conditions correspond to the conditions of beginning of the impeller gas flooding.

EXPERIMENTAL

Apparatus. The experiments were carried out in a cylindrical vessel of inside diameter $D =$ $= 0{\cdot}29$ m and height $h = 0{\cdot}7$ m whose sketch is in Fig. 2. The vessel was made of perspex and was equipped with four symmetrically placed wall baffles of width $b = 0{\cdot}03$ m along its whole height. The shaft with the impeller was located in the vertical axis of vessel, the gas was led to the aerating ring sparger placed 0·01 m under the impeller. The ring diameter was $d_d =$ $= 0{\cdot}067$ m, and the gas was dispersed through six orifices located symmetrically at the periphery of ring sparger whose diameter was 0·002 m.

The impeller used was a six plane blade impeller with its blades inclined at the angle of $\alpha = 45°$ from the vertical plane according to Czechoslovak Standard 691020 (ref.[11]) of diameter $d =$ $= 0{\cdot}096$ m. The impeller is depicted in Fig. 1. The impeller direction of rotation was of the kind that the direction of liquid flow from the impeller should be downwards. The impeller was placed at the height $H_2 = 0{\cdot}1$ m above the vessel bottom, the liquid height at rest H in the vessel was equal to the vessel diameter $D = 0{\cdot}29$ m. The temperature of water and air during experiments was 20°C.

The determination of conditions of impeller flooding was carried out from power input curves by the method described in the literature, e.g. (ref.[9]). The power input under all conditions was measured by the electrical method reported, e.g., by Strek[15] and described previously[9]. It consists in measuring the armature current of loaded and unloaded direct-current motor from which it is possible to calculate the shaft torque and from it the power input. The resulting power input is determined from the difference of power inputs of loaded and that of unloaded motor at the same impeller frequency of revolutions[16]. The experimentally found error of power input determined in this way did not exceed 3%. The frequency of impeller revolutions in experiments was within $n = 4-10\ s^{-1}$ and the gas flow rate $V_g = (0{\cdot}167-3{\cdot}5) \,.\, 10^{-4}\ m^3\ s^{-1}$.

Determination of conditions of impeller flooding. There is not a quite uniform definition of the transition between the conditions of loading and flooding; between the approaches, however, there is not a significant quantitative difference[17]. In our work we start from the conditions of the transition between both the regimes from the power input curves[9,17] in which it is assumed that it occurs under the conditions when a minimum occurs on the curves P_g/P_o vs N_F for a constant gas flow rate (values N_F change owing to the change of impeller frequency of revolutions) — see Fig. 3. The explanation is that, at the constant gas flow rate, the ascending part of the curve to the right of minimum characterizes the increase of relative power input with decreasing the impeller frequency of revolutions. For the minima on single curves (constant V_g), it is possible to read N_F, and, from it, to calculate the impeller frequency of revolutions n_c of the transition to the flooding regime of impeller at the given gas flow rate. In this way the couples of values $n_{c,exp}$ and V_g were obtained. The accuracy of quantity $n_{c,exp}$ determined in this way was $\pm 0{\cdot}5\ s^{-1}$.

This method was hitherto employed for turbine impellers where the single phases of course of the power input curve are explained by various kinds of gas cavities behind the impeller blades[18]. The situation with the inclined blade impeller is rather different as it was found by examining the two-phase flow in the impeller region with a rotating videocamera[10]: It was shown that the gas dispersion with a high-speed impeller with pumping effect downwards (axial impeller) takes place in two ways: partly by indirect loading when the gas is dispersed by the stream of liquid leaving impeller in the region under it and partly by direct loading when the gas permeates the region of blades. These situations are illustrated in Fig. 4 (ref.[10]). In case of direct loading when the gas permeates the impeller region, the greatest decrease in power input takes place. On further increasing the gas flow rate (at constant impeller frequency of revolutions) the gas gets through the impeller without dispersing, which results in increasing the relative power input. With respect to the fact that expressive minima proving this hypothesis occur on the curves of relative gassed and ungassed power input, we assume that the operating conditions of the transition from loading to flooding may be determined by the given way likewise as for the turbine impeller.

RESULTS AND DISCUSSION

The couples of values $n_{c,exp}$ and V_g for the loading/flooding transition are given in Table I. For the given gas flow rates, the values of impeller frequency of revolutions $n_{c,th}$ were calculated from Eq. (*11*) and are given in Table I as well. It is apparent from the table that the impeller frequency of revolutions corresponding to the limit of flooding read from the experiments and the revolutions calculated from Eq. (*11*) obtained from our pattern agree very well in case of lower volumetric flow rates, for

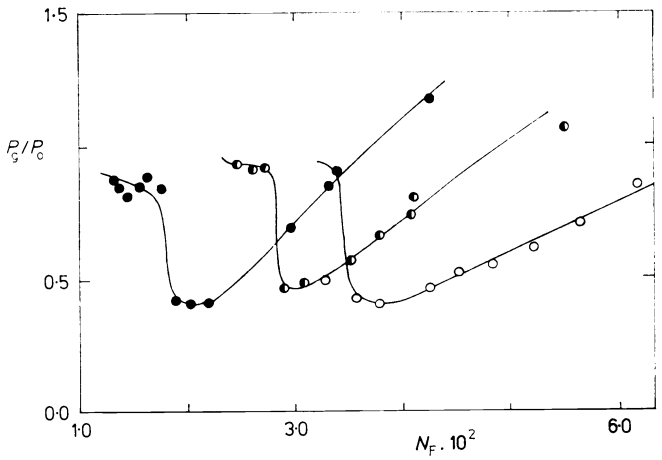

FIG. 3

The power input curves for constant gas flow rate ● $V_g = 1{\cdot}167 \cdot 10^{-4}$ m^3 s^{-1}; ◐ $V_g = 2{\cdot}167 \cdot 10^{-4}$ m^3 s^{-1}; ○ $V_g = 3{\cdot}0 \cdot 10^{-4}$ m^3 s^{-1}

higher flow rates, the deviation increases somewhat, however, does not exceed 10%. The more expressive deviations at higher flow rates are explained by increasing the bubble diameter and/or by the chain-like gas flow. Considering that the absolute value of the impeller frequency of revolutions was determined from the model and therefore that the numerical value of proportionality constant in Eq. (*11*) is derived, the results can be considered to be a verification of adequacy of the pattern. It describes the transition from the indirect to direct loading, i.e., the transition to the regime when the gas permeates the impeller region, see Fig. 4 (ref.[10]). The course of curves of relative power input from Fig. 3 is qualitatively illustrated in Fig. 5. Part of curve A corresponds to the indirect loading, the sudden decrease, segment B in Fig. 5, corresponds to the regime of gas permeation through the impeller region – according to Warmoeskerken and co-workers[10], large cavities are formed behind the impeller blades, and the impeller power input is strongly reduced. The expressive minimum on the curve, region C, can be regarded as the conditions of transition from the most effective gas dispersion (loading) to the flooding regime which takes place in the region designated by D in Fig. 5. Then it is evident from Fig. 3 that the conditions of direct loading occur in a very narrow range of operating conditions (steep decrease of power input curve, region B in Fig. 5).

It follows from the above-mentioned results that the axial high-speed impeller with pumping effect downwards is suitable for the dispersion of gases, however, it is necessary to operate in a relatively narrow range of operating conditions corresponding roughly to segment B in Fig. 5 on the relative power input curve.

In our preceding work[9], the analysis was carried out of the relations reported in literature for estimating the conditions of the loading/flooding transition. It was shown that with the invariable geometrical parameters of equipment, the relation between N_F and Fr_M, characterizing the loading/flooding transition, can be expressed by the relation between the gas flow rate and the impeller frequency of revolutions

$$n_c^A V_g^{-1} = \text{const} . \qquad (12)$$

From the equation for the inclined blade impeller (*11*) derived by us follows the relation in the form of Eq. (*12*) with the value of exponent A

$$n_c^5 V_g^{-1} = \text{const} . \qquad (13)$$

In paper[9], exponent A was reported for three different agitating arrangements: $A \cong 3$ for one Rushton turbine, $A \cong 3{\cdot}4$ for two-impeller arrangement with two Rushton turbines, and $A \cong 4$ for two-impeller arrangement with one Rushton turbine (lower impeller) and with an inclined blade impeller pumping the liquid upwards (upper impeller). For one axial impeller used in this work is consequently $A = 5$. The higher value of exponent A gives evidence of higher sensitivity to the

TABLE I

Dependence between the gas flow rate and the impeller critical frequency of revolutions for the impeller loading/flooding transition[a]

$V_g \cdot 10^4$ / $m^3\ s^{-1}$	$N_{F,exp} \cdot 10^2$	$n_{c,exp}$ / s^{-1}	$n_{c,th}$ / s^{-1}
0·167	0·475	4·0	4·62
0·333	0·750	5·0	5·30
0·500	1·025	5·5	5·75
0·667	1·250	6·0	6·09
0·833	1·450	6·0	6·37
1·000	1·725	6·5	6·61
1·167	1·875	7·0	6·81
1·500	2·121	7·5	7·16
1·833	2·590	8·0	7·45
2·167	2·885	8·5	7·71
2·500	3·308	8·5	7·93
3·000	3·775	9·0	8·23
3·500	4·150	9·5	8·49

[a] Six inclined ($\alpha = 45°$) plane blade impeller[11], $d/D = H_2/D = 0{\cdot}1$; $H/D = 1$, $b/D = 0{\cdot}1$; $Re_M > 1{\cdot}0 \cdot 10^3$.

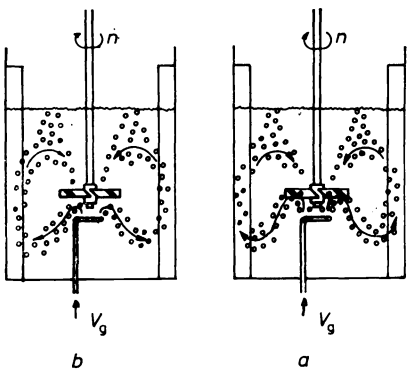

FIG. 4

Direct an indirect loading: *a* direct loading; *b* indirect loading

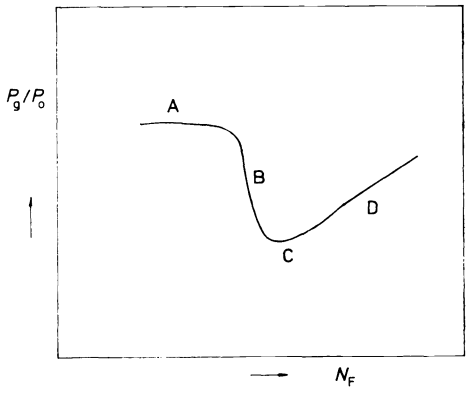

FIG. 5

Typical shape of relative power input, P_g/P_o, dependence on gas flow number, N_F, ref.[10]; (A indirect loading, B presence of large cavities behind the blades of stirrer, C direct loading, D flooding of the stirrer)

operating conditions during the loading/flooding transition. Equation (*11*) can be transferred to the relation between the flow-rate and Froude numbers for mixing with the following result:

$$V_g/n \sim n_c^4 \tag{14}$$

$$N_F \sim Fr_M^2 . \tag{15}$$

It is possible to enumerate also the proportionality constant in these relations. It is, however, valid only for our size of mixing equipment. Moreover, relation (*15*) is valid only for dispersing gas with axial high-speed impeller with pumping effect downwards and determines the relation between n and V_g for the impeller loading/flooding transition.

CONCLUSIONS

From the equilibrium of forces acting on a gas bubble in the region under inclined blade impeller with downwards pumping effect, the relation was derived between the gas flow rate and the impeller frequency of revolutions characterizing the transition between the loading and flooding conditions (Eq. (*11*)). The conditions of the impeller loading/flooding transition obtained experimentally from the curves of relative power input were found to be in good agreement with those determined from derived equation (*11*). It has followed from the experiments that the axial high-speed impeller is suitable for the gas dispersion, however, it is more sensitive to the maintainance of suitable operating conditions in comparison with the radial high-speed impellers.

SYMBOLS

A	constant in Eq. (*12*)
b	baffle width, m
C_P	constant in Eq. (*4*)
d	impeller diameter, m
d_b	bubble diameter, m
d_d	diameter of ring sparger, m
D	vessel diameter, m
g	acceleration of gravity, m s^{-2}
h	vessel height, m
H	liquid height in vessel at rest, m
H_2	impeller height above bottom, m
n	impeller frequency of revolutions, s^{-1}
n_c	impeller critical frequency of revolutions characterizing impeller loading/flooding transition, s^{-1}
$n_{c,exp}$	impeller critical frequency of revolutions determined experimentally, s^{-1}
$n_{c,th}$	impeller critical frequency of revolutions determined by calculation, s^{-1}

P_g gassed impeller power input, W
P_o ungassed impeller power input, W
S impeller cross-sectional area, m^2
V_g gas (air) flow rate, $m^3\ s^{-1}$
V_P volumetric flow rate of liquid through impeller (impeller pumping capacity), $m^3\ s^{-1}$
Fr_M $= n^2d/g$ Froude number for mixing
N_F $= V_g/(nd^3)$ flow rate number
Re_b $= \omega d_b/\nu$ Reynolds number for liquid flowing around bubble
Re_M $= nd^2/\nu$ Reynolds number for mixing
α angle of inclination of impeller blade, °
ψ drag coefficient for liquid flowing around bubble
ν kinematic viscosity of liquid, $m^2\ s^{-1}$
ϱ_l liquid density, $kg\ m^{-3}$
ϱ_g gas density, $kg\ m^{-3}$
ω mean velocity of liquid streaking from impeller rotor region, $m\ s^{-1}$

REFERENCES

1. Oldshue J. Y.: Chem. Eng. Prog. *85*, 33 (1989).
2. Meyer H. P.: Swiss Biotechnol. *6* (4), 27 (1988).
3. Fořt I. in: *Mixing. Theory and Practice* (V. W. Uhl and J. B. Gray, Eds), Vol. III. Academic Press, New York 1986.
4. Cooke M.: Chem. Eng. *456*, 39 (1989).
5. Toma M. K., Ruklish M. P., Viestours U. E., Rikmanis M. A., Vanage J. J.: Izv. Akad. Nauk Latv. SSR *8* (481), 93 (1987).
6. Mikulcová E., Kudrna V., Vlček J.: Sb. Vys. Sk. Chem.-Technol. Praze, K *1*, 167 (1967).
7. Smith J. M., Warmoeskerken M. M. C. G.: *Proc. 5th Europ. Conference on Mixing, Würzburg 1985*; p. 115.
8. Nienow A. W., Konno M., Warmoeskerken M. M. C. G., Smith J. M.: *Proc. 5th Europ. Conference on Mixing, Würzburg 1985*; p. 143.
9. Machoň V., Vlček J., Skřivánek J.: *Proc. 5th Europ. Conference on Mixing, Würzburg 1985*; p. 155.
10. Warmoeskerken M. M. C. G., Speur J., Smith J. M.: Chem. Eng. Commun. *25*, 11 (1984).
11. *Czechoslovak Standard 69* 10 20. VÚCHZ — CHEPOS, Brno 1969.
12. Medek J., Fořt I.: Chem. Prum. *29/54*, 2 (1979).
13. McCabe W. L., Smith J. C.: *Unit Operations of Chemical Engineering*. McGraw-Hill, New York 1976.
14. Clift R., Grace J. R., Weber M. E.: *Bubbles, Drops and Particles*. Academic Press, New York 1978.
15. Strek F.: *Míchání a míchací zařízení*. SNTL, Praha 1977.
16. Machoň V., Vlček J., Hudcová V.: *Proc. 6th Europ. Conference on Mixing, Pavia (Italy) 1988*; p. 351.
17. Nienow A. W., Wisdom D. J., Middleton J. C.: *Proc. 2nd Europ. Conference on Mixing, Cambridge 1977*; p. F1.
18. Bruijn W., Van't Riet K., Smith J. M.: Trans. Inst. Chem. Eng. *52*, 88 (1974).

Translated by J. Linek.